Extraction of New Applicable Dimensionless Relations in the Wedge Impact Problem Using WCSPH Method

Jafar Gerdabi, Amir H. Nikseresht
and Mohammad A. Esmaeili-Sikarudi*

Department of Mechanical Engineering, Shiraz University of Technology, Shiraz, Iran
E-mail: m.aminesmaili.s@gmail.com
**Corresponding Author*

Received 08 June 2021; Accepted 08 October 2021;
Publication 10 November 2021

Abstract

Impact problem associated with water entry of a wedge has important applications in various aspects of naval architecture and ocean engineering. In the present study, the 2DOF (2 Degrees of Freedom) wedge impact problem into the water with various wedge deadrise angles and impact velocities is investigated using Weakly Compressible Smoothed Particle Hydrodynamics (WCSPH) method. Artificial viscosity and density correction are used to create stability and also to prevent the penetration of fluid particles into the solid boundary. Solving the impact problem is very time-consuming, therefore extracting new mathematical relations can be very useful to calculate some important and applicable parameters in a certain range of wedge angles and impact velocities. In the present research, some new dimensionless applicable relations using the Buckingham π theorem are extracted to investigate important parameters such as acceleration and slamming force in general cases of a wedge impact problem. Then, these mathematical relations are validated by the results obtained from the simulations.

European Journal of Computational Mechanics, Vol. 30_4–6, 305–336.
doi: 10.13052/ejcm2642-2085.30462

Keywords: WCSPH method, wedge impact, artificial viscosity, density correction, slamming coefficient, kernel functions, mathematical relations, Buckingham π theorem.

1 Introduction

The study of water impact is one of the complicated problems in various fields of engineering especially in ocean engineering and naval architecture. One of the main concerns is to calculate the impact force which is exerted on the floating bodies in the water entry impact problem using dynamic equations of motion [1]. The impact of flying boats, seaplanes, and speedboats on the sea surface can be roughly modeled as a wedge impact problem into the water.

The water impact problem was first investigated by Von Karman (1929) [2]. He used the momentum and the added mass theory to estimate the impact force during a seaplane landing without considering the effect of water pile-up during impact. Wagner [3] developed Von Karman's analysis by taking into account the effect of water pile up during the impact phenomenon. Dobrovol'skaya [4] used similarity flow solutions for wedges. Divitiis and de Socio [5] used a physico-mathematical model of a potential singularities distribution together with the solution of the nonlinear free-surface problem. Korobkin [6] improved the impact force prediction by using the higher-order terms in the Bernoulli equation together with the generalized Wagner model and the Logvinovich model [7] and compared the results with experiments. Also, he showed that the Logvinovich model has better results.

Solving this problem using the mesh-based Eulerian-Lagrangian methods is cumbersome and time-consuming. The experimental studies are also expensive, thus obtaining some mathematical relations to calculate the maximum acceleration of the wedge and the impact force which is exerted on the wedge is very useful to save time and expenses. In the present study, the simulation results of the WCSPH method are used to derive general mathematical relations for calculating the force which is exerted on a wedge impacting into the water. Smoothed particle hydrodynamics was proposed by Luci [8], Gingold, and Monaghan [9] in 1977. This method was firstly used for simulating astrophysical phenomena such as star formation. This method developed and extended to other applications gradually until the 21st Century [10–20].

Yettou et al. [21] conducted an experimental study to investigate the water impact of the symmetrical wedge in 2006. Oger et al. [22] simulated the wedge water entry using the WCSPH method in 2006. They calculated the

force exerted on the wedge by projecting the particles on the wedge surface and also they used pressure interpolation to calculate the pressure on the particles of the wedge surface. Kai et al. [23] and Gong et al. [24] simulated the wedge water entry with the WCSPH method, but they calculated the pressure on the wedge surface using an equation of state and also the non-reflective boundary treatment in 2009 and 2011 respectively. Gong et al. investigated the impact problem at different velocities, from 2 m/s to 7 m/s. In 2013, Koukouvinis et al. [25] used the SPH-ALE[1] method to simulate a 2D wedge water entry problem. The SPH-ALE method was firstly introduced by Vila [26]. In this method, the Eulerian forms of the conservation laws are combined with the Lagrangian forms. Sun [27] simulated the wedge impact problem for several different wedge masses, deadrise angles, and impact velocities using the SPH method. Farsi and Ghadimi [28] simulated the wedge impact problem at deadrise angels between 10° and 81° using the SPH method. Amicarelli et al. [29] simulated a 2D symmetric and asymmetric wedge water impact problem using the WCSPH method. They used the boundary force proposed by Monaghan for calculating the force exerted on the wedge surface. Also, Chen and Li [30] used a repulsive force relation to calculate the force exerted on the wedge surface in 2016. Cheng et al. [31] used a higher-order boundary element method (HOBEM) for the investigation of wedge water impact in the presence of waves in 2018. In 2019, Chen et al. [32] studied wedge-water entry near a single piece of ice using computational fluid dynamics and a Wagner type theoretical model. Wen et al. [33, 34] studied the wedge impact problems with varying speed in 2020 and 2021. They observed a linear relationship between the pressure coefficient and a dimensionless variable from which they derived an approximate solution for wedge impact with several deadrise angles. These studies included numerical (VOF) and theoretical methods to provide a fast and accurate prediction of the pressure on wedge surfaces.

In this study, the experimental and numerical results of Zhao et al. [35] are used to validate the results.

In the present research, an in-house C++ code that is based on the WCSPH method is prepared and validated using the experimental data of the under-gate flow problem. Also, the wedge water impact problem is simulated and validated. Moreover, the effects of different wedge deadrise angles (between 15° and 60°) and also different impact velocities (between 6.16 m/s and 14.73 m/s) are investigated. It should be mentioned that in all

[1] Arbitrary Lagrangian Eulerian.

simulations the wedge mass is 241 kg. The main goal of the present research is to introduce some applicable relations using new dimensionless parameters to express the important parameters such as acceleration and slamming force in the general case of the wedge impact problem.

2 WCSPH Method

There are several methods for discretizing the governing equations in the WCSPH method. In the present study, Equations (1) and (2) are used for discretizing continuity and momentum equations respectively [22]:

$$\frac{D\rho_i}{Dt} = \sum_j m_j \vec{u}_{ij} \cdot \nabla_i W_{ij} \tag{1}$$

$$\frac{D\vec{u}_i}{Dt} = -\sum_j m_j \left(\frac{p_i}{\rho_i^2} + \frac{p_j}{\rho_j^2} + \Pi_{ij} \right) \nabla_i W_{ij} + \vec{g} \tag{2}$$

where $\vec{u}_{ij} = \vec{u}_i - \vec{u}_j$, m and Π are the particle mass and the artificial viscosity respectively. The index j is related to the neighbor particles.

Artificial viscosity in the form of Equation (3) is used to reduce the numerical noise and unphysical oscillations [23]:

$$\Pi_{ij} = \begin{cases} \dfrac{-\alpha_\pi \overline{c_{ij}} \mu_{ij}}{\overline{\rho_{ij}}} & \vec{u}_{ij} \cdot \vec{r}_{ij} < 0 \\ 0 & \vec{u}_{ij} \cdot \vec{r}_{ij} \geq 0 \end{cases} \tag{3}$$

where μ_{ij} and k_i are calculated according to Equations (4) and (5).

$$\mu_{ij} = h \frac{k_i + k_j}{2} \frac{\vec{u}_{ij} \cdot \vec{r}_{ij}}{\vec{r}_{ij}^2 + \eta^2} \tag{4}$$

$$k_i = \frac{|div(\vec{u}_i)|}{|div(\vec{u}_i)| + \sqrt{Sr_i : Sr_j} + 10^{-4} c_i / h} \tag{5}$$

In general, $\vec{f}_{ij}$ and $\overline{f_{ij}}$ is considered as $\vec{f}_i - \vec{f}_j$ and $(f_i + f_j)/2$, respectively. Also, $\alpha_\pi = 0.04$ and $\eta = 0.1\ h$ and Sr is the shear rate stress tensor.

In the WCSPH method, fluid is considered as a weakly compressible fluid, and pressure is calculated using the following equation of state [36]:

$$P = \kappa \left[\left(\frac{\rho}{\rho_0} \right)^\gamma - 1 \right] \tag{6}$$

where $\kappa = \rho_0 c_0^2/\gamma$, $\gamma = 7.0$, $c_0 = 10\ U_W$ and U_W is of the order of the maximum possible velocity of particles [23]. c_0 has a direct effect on the fluid compressibility and time step.

To move the particles and also to smooth the noise inherent in the WCSPH method, Equation (7) which is called the XSPH method [23] is used.

$$\left[\frac{d\vec{r}}{dt}\right]_i = \vec{u}_i - \varepsilon \sum_j m_j \frac{\vec{u}_{ij}}{\overline{\rho_{ij}}} W_{ij}, \quad \varepsilon = 0.5 \tag{7}$$

The modified cubic spline kernel function (Equation (8)) is used in this study. This kernel function exhibits better stability than the simple cubic spline kernel function [37].

$$W(r,h) = \alpha_d \begin{cases} q^3 - 6q + 6 & 0 < r < h \\ (2-q)^3 & h \le r \le 2h \\ 0 & r \ge 2h \end{cases} \tag{8}$$

where $q = |\vec{r}_{ij}|/h$ and $\alpha_d = 1/(3\pi h^2)$.

Choosing a suitable time step is particularly important, because using an inappropriate time step, leads to particle instability and solution divergence. The time step should be small enough to prevent numerical instability [38]. The stability conditions regarding viscosity and inertia are satisfied according to Equation (9) [39].

$$\Delta t = 0.10 \min\left(\frac{h}{c_{max} + u_{max}}, \left(\frac{h}{f_{i,max}}\right)^{0.5}, \frac{h^2}{\upsilon}\right) \tag{9}$$

The parameters c_{max}, u_{max} and f_i are the maximum sound speed, the maximum velocity, and acceleration of the particles.

Since the WCSPH method is prone to pressure noise, the density correction method should be used to obtain a smooth pressure field. Equations (10) and (11) lead to a zeroth-order density correction which means a constant density can be captured accurately [40].

$$\rho_i^{new} = \sum_j m_j \tilde{W}_{ij} \tag{10}$$

$$\tilde{W}_{ij} = \frac{W_{ij}}{\sum_j W_{ij} \frac{m_j}{\rho_j}} \tag{11}$$

A repulsive force as in Equation (12) which is proposed by Monaghan is used to prevent fluid particles from entering the solid boundaries [19].

$$f(\vec{r}) = \begin{cases} D_0 \left(\left(\frac{r_0}{|\vec{r}|} \right)^{p_1} - \left(\frac{r_0}{|\vec{r}|} \right)^{p_2} \right) \frac{\vec{r}}{|\vec{r}|^2} & |\vec{r}| < r_0 \\ 0 & |\vec{r}| \geq r_0 \end{cases} \tag{12}$$

where $p_1 = 12$, $p_2 = 6$ and $D_0 = gH$.

The initial space between particles is r_0, H is the depth of the still water and g is the gravity acceleration.

This repulsive boundary condition is used in the wedge water entry test cases. For the under-gate flow test cases, the image boundary condition is used [39]. Using Equation (13) the hydrostatic pressure field can be imposed on the fluid particles initially.

$$\rho = \rho_0 \left(1 + \frac{\gamma g h(z)}{c_0^2} \right)^{1/\gamma} \tag{13}$$

ρ_0 is the initial density of the fluid and $h(z)$ is the depth of each particle below the free surface [19].

The predictor-corrector time advancing algorithm is used and at first, the velocity, density, and position are calculated for the time $\Delta t/2$, and afterward, the velocity, density, and position of the particles are corrected for the time $t + \Delta t/2$. Therefore, a second-order solution in time is obtained [40]. The pressure at the boundary surface of the wedge is calculated by interpolating the pressure of fluid particles adjacent to the wedge. From the pressure distribution, the force exerted on the wedge, the acceleration, the velocity, and the position of the wedge are calculated [22].

The slamming coefficient in the wedge-water impact problem is defined as in Equation (14):

$$Cs = \frac{2F}{\rho_0 V_w^2 L_w} \tag{14}$$

where L_w is the width of the wedge base, V_w is the wedge impact velocity and F is the total force exerted on the wedge.

3 Dimensionless Relations

In general, there are three primary dimensions including mass (M), time (T), and length (L) in impact problems. To use the Buckingham π theorem,

Table 1 Dimensions of related parameters in wedge impact problems

Parameter	a	V_w	$L_w,\ H_w$	m	ρ	t	θ	F
Dimension	LT^{-2}	LT^{-1}	L	M	ML^{-3}	T	$-$	MLT^{-2}

all parameters involved must be written in the form of these three primary dimensions. It should be noted that in the present study, wedge mass is fixed and is not used in any relations. Table 1 shows all important parameters in terms of primary dimensions.

It should be noted that θ is a dimensionless parameter and $\tan(\theta)$ relates the wedge base (L_w) and the wedge height (H_w). In the following, several mathematical relations are extracted using the Buckingham π theorem considering the effect of parameters on each other. In short, there are two general conditions:

1. The impact velocity is directly related to the maximum acceleration and is inversely related to the time of maximum force on the wedge.
2. The size of the deadrise angle is directly related to the time of maximum force on the wedge and is inversely related to the maximum acceleration.

In short, if the impact velocity increases, the maximum acceleration also increases, but the time of maximum force on the wedge decreases. Also, increasing the deadrise angle makes the wedge sharp, so that it can enter the water more easily. Therefore, the maximum acceleration on the wedge decreases, and the time of the maximum force on the wedge increases.

3.1 Non-dimensional Acceleration

In this study, the symmetrical impact problem is investigated, so the horizontal acceleration is calculated close to zero. Also, since the wedge mass is fixed, so the wedge mass does not enter into relations.

Acceleration is one of the dependent parameters which depends only on the impact velocity and the geometry of the wedge such as the deadrise angle, wedge base, and wedge height. On the other hand, it is clear that $H_w = L_w \tan(\theta)/2$. Therefore, Equation (15) can be written for acceleration:

$$a = f(L_w,\ V_w, \theta) = f(H_w, V_w) \tag{15}$$

Therefore, dimensionless acceleration can be represented by Equation (16):

$$a^* = aH_W^i V_W^j \rightarrow (L^0T^0) = (LT^{-2})(L)^i(LT^{-1})^j \tag{16}$$

where i and j are unknowns which must be calculated by equating the exponents of L and T.

Finally, i and j are obtained as 1 and -2, respectively, so the general form of the dimensionless acceleration is as follows:

$$a^* = aH_w V_W^{-2} = \frac{aH_w}{V_W^2} = \frac{aL_w}{2V_W^2}\tan(\theta) \tag{17}$$

It should be noted that the parameter a is the total vertical acceleration of the wedge which is equal to -9.81 m/s^2 before the impact. To start a^* from zero, a is replaced by $a + |g|$, so that the dimensionless acceleration a^* is due to the hydrodynamic force which is exerted on the wedge by the fluid and is as follows:

$$a^* = \frac{(a + |g|)L_w}{2V_w^2} tan(\theta) \tag{18}$$

3.2 New Dimensionless Force Coefficient

The slamming coefficient is a dimensionless force coefficient but depends on the deadrise angle. It is necessary to define a new dimensionless force coefficient that is independent of the deadrise angle. According to the second condition in Section 3, the size of the deadrise angle is inversely related to the maximum acceleration and therefore to the force exerted on the wedge. Therefore a new dimensionless relation is created by multiplying the slamming coefficient by $tan(\theta)$ as in Equation (19). Moreover, this new dimensionless relation is very useful, as shown in the results section later.

$$Cs^* = Cstan(\theta) = \frac{2F}{\rho_0 V_w^2 L_w} tan(\theta) \tag{19}$$

F is the total force exerted on the wedge and ρ_0 is the initial density.

3.3 Non-dimensional Time

Similar to acceleration, another dependent parameter can be time and is shown as Equation (20):

$$t = f(L_w, V_w, \theta) = f(H_w, V_w) \tag{20}$$

Using Table 1, dimensionless time can be represented by Equation (21):

$$t^* = tH_W^i V_W^j \rightarrow (L^0 T^0) = (T)(L)^i (LT^{-1})^j \tag{21}$$

By equating the exponents of L and T, i and j are obtained to be -1 and 1, respectively, so the general form of the dimensionless time is as follows:

$$t^* = \frac{tV_w}{H_w} = \frac{2tV_w}{L_w tan(\theta)} \tag{22}$$

Constant numbers in dimensionless relations can be removed without any problems as in Equation (23):

$$t^* = \frac{tV_w}{L_w tan(\theta)} \tag{23}$$

4 Results and Discussion

4.1 Validation

In this study, the two test cases of under-gate flow and wedge water entry are used to validate the code and simulations.

The under-gate flow problem is of importance due to the study of wave behavior and free surface dynamics. The under-gate flow test case consists of a water column with a non-dimensional height and width of 1 which flows under a gate with a height of 0.2357. Figure 1 shows the profile of a fluid free surface and it is consistent with the results of the finite volume method using the VOF scheme to track the free surface profile [41].

The non-dimensional length, height, time, and pressure are calculated using $X^* = x/L$, $Z^* = z/H$, $T^* = t(c_0/H)$ and $P^* = P/(\rho g H)$

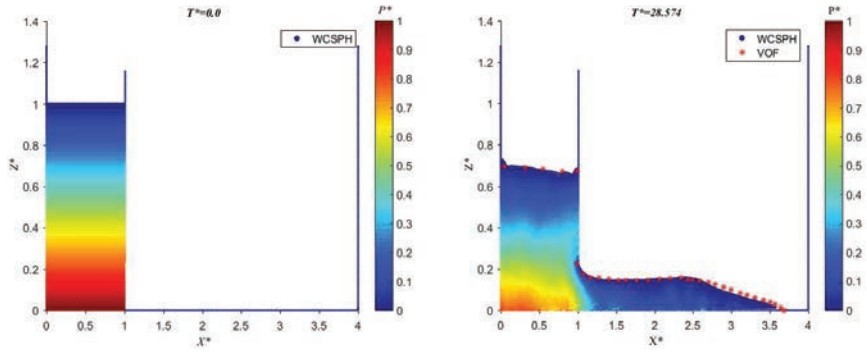

Figure 1 Comparison of the free surface in fluid flow under the gate using the WCSPH method and the VOF [41] method.

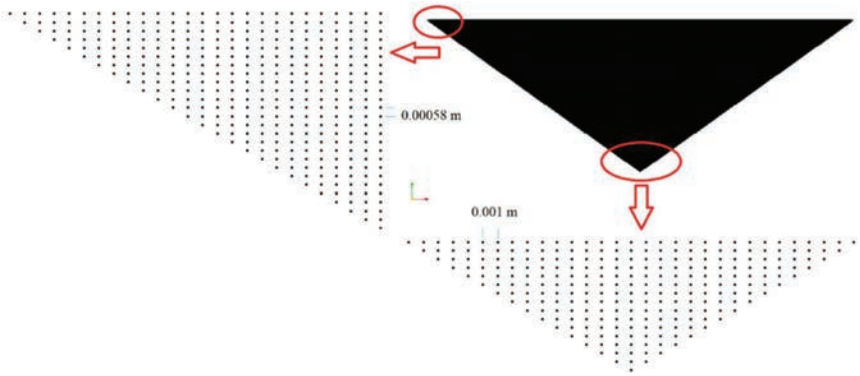

Figure 2 Geometry of a wedge with 30° deadrise angle along with the initial distance of particles.

respectively, where, H is the initial height and L is the initial width of the water column.

The second problem which is used to validate the code is the wedge-water impact problem. The total number of particles used in this case is equal to 2949002, of which 63001 particles belong to the wedge geometry. The initial distance between the fluid particles is very important in the SPH method, and selecting an inappropriate value for this parameter causes instability and divergence in the solution. Figure 2 shows a wedge with 30° deadrise angle and the initial distribution of fluid particles with a constant distance equal to 0.001 m. The distance between vertical and horizontal particles on the wedge is not the same and is 0.00058 m and 0.001 m, respectively. The wedge has two degrees of freedom and can move vertically and horizontally.

In the present study, the wedge impact problem in a 2.4 m wide reservoir with a water depth of 1.2 m is investigated. The weight of the wedge is 241 kg and the base length of the wedge is 0.5 m. The wedge deadrise angle is $\pi/6$ and its impact velocity is 6.15 m/s. The initial wedge velocity is set to 6.09 m/s, and the wedge tip is initially 0.04 m above the free surface. Therefore, the wedge velocity reaches 6.15 m/s when it impacts the water surface. Also, the speed of sound is set to 61.5 m/s based on $c_0 = 10\, U_W$. It should be noted that the force exerted on the wedge is calculated for a wedge with 0.2 m depth as in experiments [35]. Figure 3, shows the initial hydrostatic pressure distribution in the water.

Figure 4 shows the dimensionless acceleration-time curves of the wedge motion for three different initial fluid particles distance and is compared with the numerical method (B.E.M) and experimental results of [35]. The figure

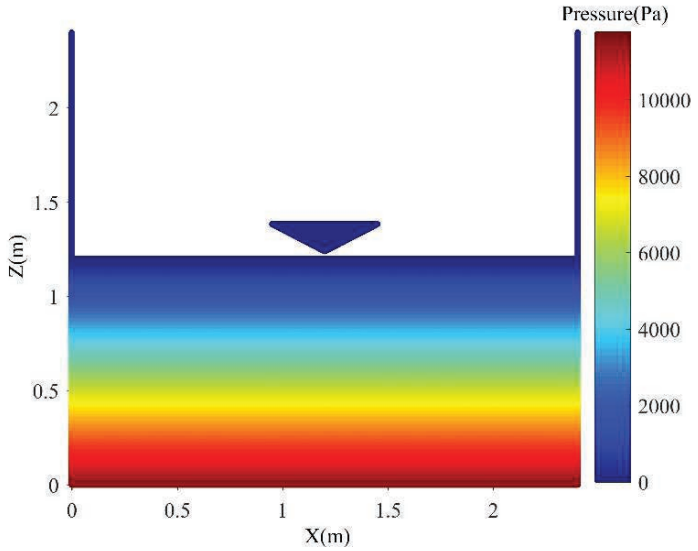

Figure 3 The initial hydrostatic pressure distribution at time zero.

shows that at the initial distance of the fluid particles equal to 0.003, there is a large fluctuation in acceleration, but reducing the distance eliminates the oscillations, but the maximum amount of acceleration in the three curves is almost the same. Therefore, a distance of 0.001 is a suitable distance, and therefore in all simulations, the initial distance of the fluid particles is set to 0.001 m.

At first, the wedge falls freely therefore its acceleration is equal to the gravity acceleration which is downward and assumed to be negative. When the wedge impacts the water surface, an upward force is exerted on it and it causes firstly that the wedge acceleration decreases in a very short time and reaches zero. After that, the direction of the acceleration changes from negative to positive, and also the acceleration can increase in a positive direction.

As it is depicted in Figure 4, the B.E.M. [35], and the present numerical results are coincident with each other at the start and end of the time interval and the maximum difference is at dimensionless time 0.34.

After this time, the difference between numerical and experimental results increases because of the three-dimensional effects which are shown in [42]. The WCSPH method is prone to noise in the calculation of density which makes the numerical results noisy. In this study this unphysical noise is removed as far as it is possible, using the density correction techniques.

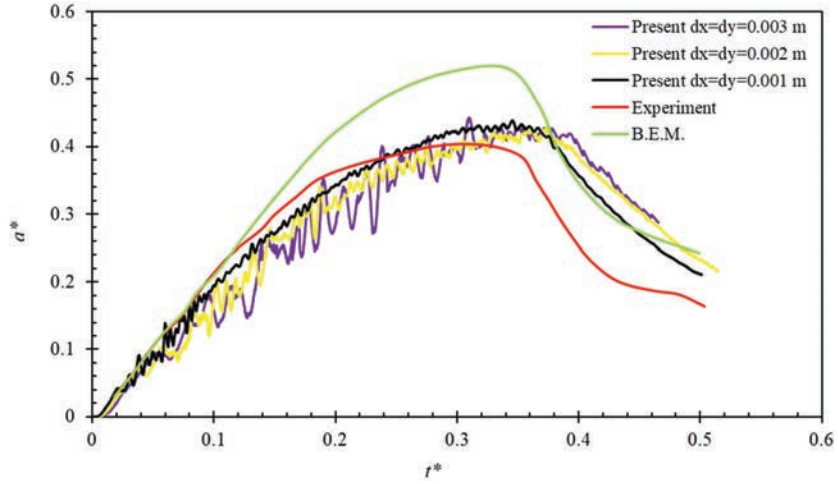

Figure 4 Comparison of the present dimensionless acceleration-time results using different initial fluid particles distances with experimental and B.E.M. results of [35].

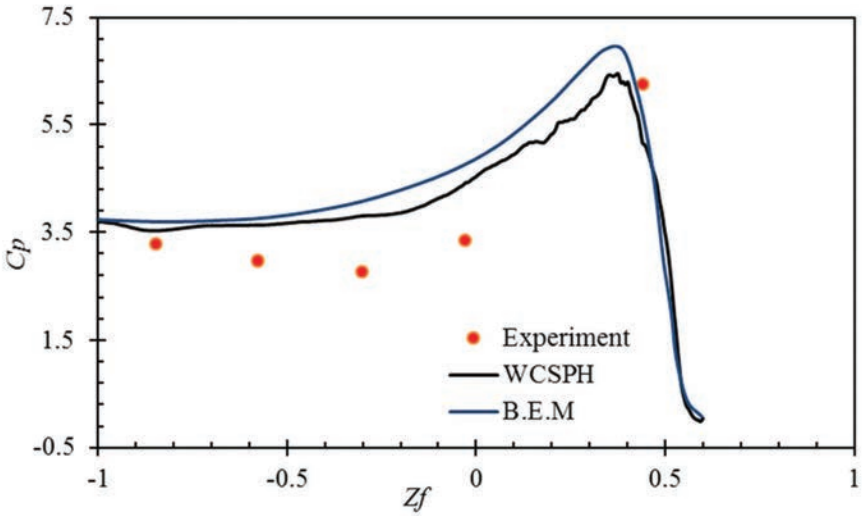

Figure 5 Comparison of the present results for the pressure coefficient on the wedge surface at the dimensionless time of 0.34 with the experimental and B.E.M. results of [35].

The pressure coefficient at the dimensionless time of 0.34 is compared with the numerical (B.E.M) and experimental results of [35] in Figure 5. It shows that in maximum value the result of the WCSPH method coincides with the experimental value well.

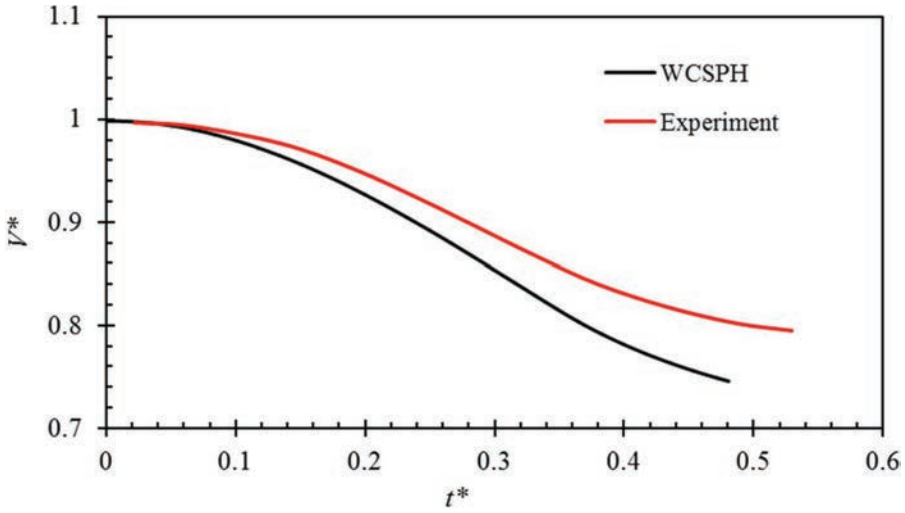

Figure 6 Comparison of the present vertical velocity versus time with experimental ones [35].

The non-dimensional pressure coefficient and the parameter Zf are calculated using Equations (24) and (25). When the parameter Zf is equal to -1 it refers to the tip of the wedge and when it equals to 0 it refers to the points on the lateral edges where the water free surface contacts with the wedge also, $Zf > 0$ refers to the parts of the wedge which are out of the water.

$$C_p = \frac{P}{0.5\rho_0 {V_w}^2} \tag{24}$$

$$Zf = \frac{z}{\int_0^t V_t(t)dt} \tag{25}$$

The variable $V_t(t)$ is the velocity of the wedge at each time instant. Figure 6 shows the non-dimensional vertical velocity ($V^* = V/V_w$) versus time which is compared with the experimental results of [30].

As time proceeds, the difference between numerical values and experimental results increases, mainly due to the three-dimensional effects. In three dimensions, after the wedge impacts into the water, fluid particles are thrown away from four sides of the wedge but in 2-D simulations, it occurs only from two sides of the wedge. This means that fluid has more freedom in 3-D to escape from the wedge during the impact problem which leads to a smaller slamming force and higher wedge velocity.

4.2 The Effect of Different Wedge Deadrise Angles

In this section the effect of four wedge deadrise angles of $\pi/12$, $\pi/6$, $\pi/4$ and $\pi/3$ on pressure, acceleration, and force coefficient are investigated for the wedge impact velocity of 6.18 m/s. Also, some general mathematical relations are derived for the calculation of the peak acceleration and force coefficient. The free surface profile and pressure contours during the impact problem of a wedge with different wedge deadrise angles and also different wedge velocities are depicted in Appendix 1. As it is obvious from these figures if the wedge deadrise angle reduces or the impact velocity increases, the pressure distribution around the wedge and the force which is exerted on the wedge increase. The fluid particles escape tangential from the lateral edges of the wedge. This phenomenon causes some particles to go away from the other fluid particles, therefore there are not enough particles in their neighborhood and the density cannot be calculated correctly. This is shown in figure (a) of Appendix 1. Figure 7. Shows the dimensionless acceleration

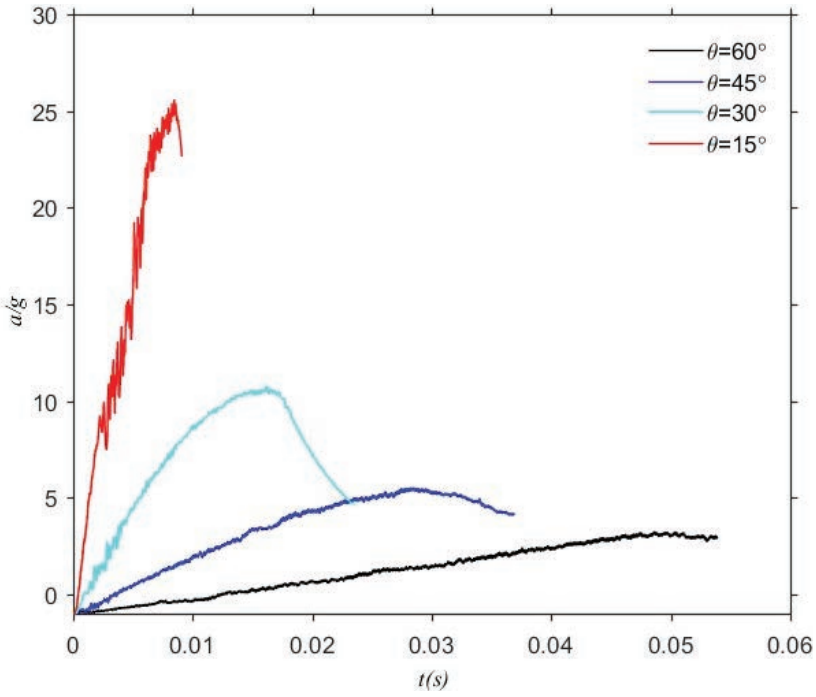

Figure 7 Dimensionless acceleration versus time for different wedge deadrise angles in the impact velocity of 6.18 m/s.

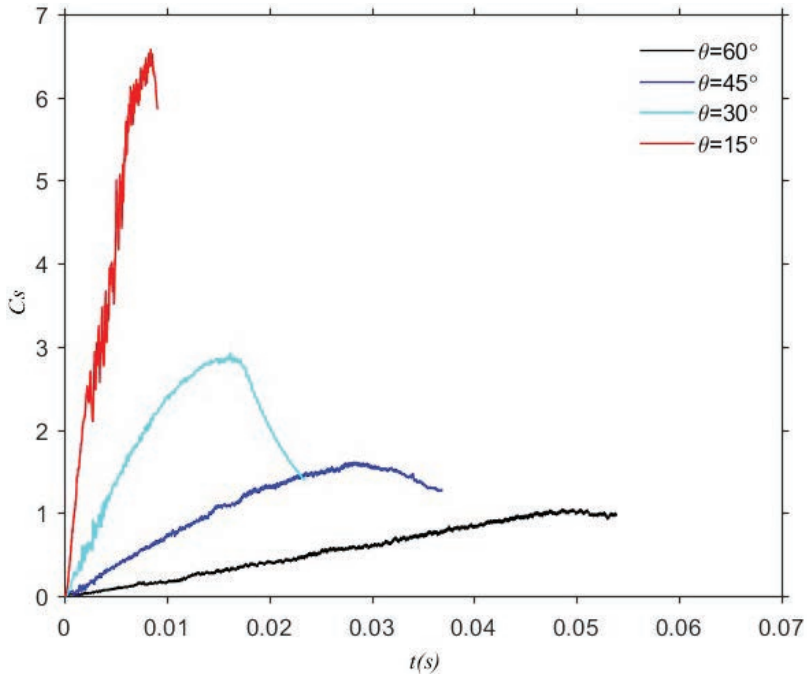

Figure 8 Slamming coefficient versus time for different wedge deadrise angles in the impact velocity of 6.18 m/s.

versus time for different wedge deadrise angles at the same impact velocity of 6.18 m/s. As the wedge deadrise angle reduces, both acceleration and force increase, and their behaviors are much noisier. As the wedge deadrise angle decreases the wedge shape resembles more to a flat plate; hence, the wedge cannot enter into the water easily, and therefore, the impact pressure and force increase. As mentioned before the WCSPH method is prone to noise in density calculation since the fluid is assumed to be slightly compressible. To reduce noise, the sound speed should be set so that the density variation remains less than one percent. Figure 8 shows the slamming coefficient for the different wedge angles when the wedge impact velocity is 6.18 m/s. When the force increases, the wedge velocity decreases, and the slamming coefficient increases according to Equation (14).

Using the new dimensionless form of acceleration and time as in Equations (18) and (23), Figure 7 can be re-sketched as shown in Figure 9. It is depicted in Figure 9 that using these new dimensionless parameters causes all curves of acceleration for different wedge angles to coincide with each

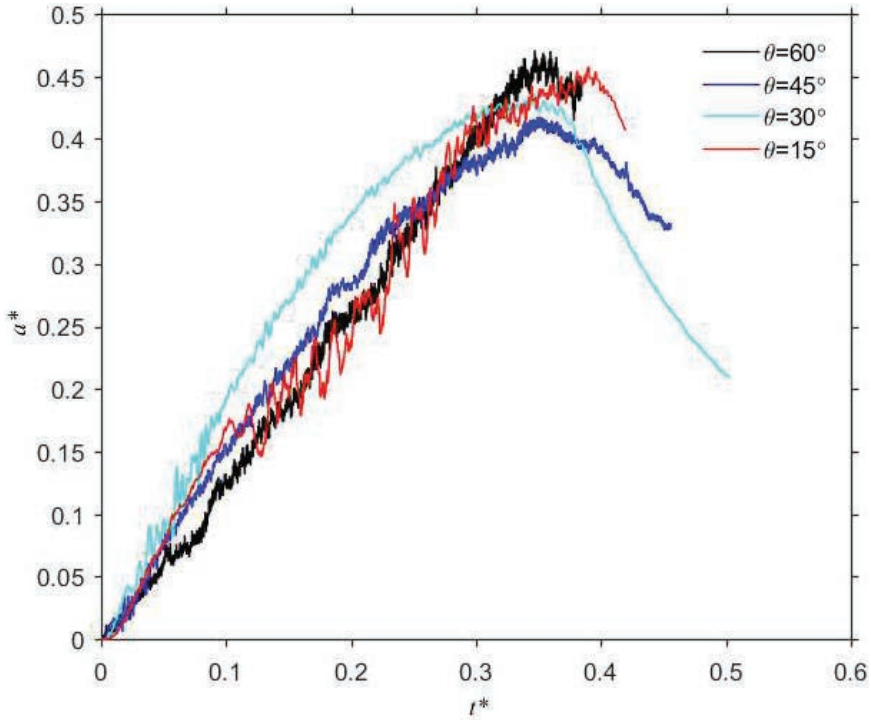

Figure 9 New dimensionless acceleration versus dimensionless time for different wedge deadrise angles in the impact velocity of 6.18 m/s.

other approximately and the dimensionless parameters are independent of the wedge angles. Also using Equations (19) and (23), Figure 8 can be re-sketched as shown in Figure 10.

The maximum force, acceleration, and impact force coefficient which is exerted on the wedge and also the time related to the maximum force are provided in Table 2.

Calculating the maximum impact force in the wedge water entry is one of the most important problems in ocean engineering and naval architecture; hence, in this section, it is tried to implement practical relations to estimate the peak loads in the impact problem without needing cumbersome simulations.

Table 2, shows that the wedge deadrise angle has no significant effect on the maximum impact force coefficient, maximum acceleration, and the time related to these values. Therefore, the average of each column can be accepted as a single value for the maximum acceleration, maximum impact

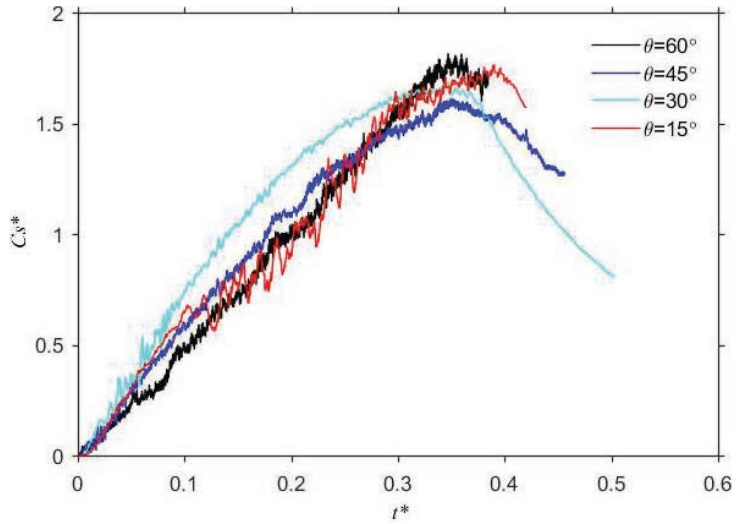

Figure 10 New impact force coefficient versus dimensionless time for different wedge deadrise angles in the impact velocity of 6.18 m/s.

Table 2 Maximum force, impact force coefficient, dimensionless acceleration, and the dimensionless time of the maximum force at the impact velocity of 6.18 m/s

θ°	t_p^*	$F(kN)$	Cs_{max}^*	a_{max}^*
15	0.390	12.575	1.765	0.457
30	0.346	5.56	1.68	0.436
45	0.350	3.074	1.61	0.417
60	0.347	2.00	1.815	0.470

force coefficient and the related time with a reasonable error in the impact velocity of 6.18 m/s and are as follows:

$$a_{max}^* \approx 0.445 \pm 6.7\% \tag{26}$$

$$Cs_{max}^* \approx 1.7175 \pm 6.8\% \tag{27}$$

$$t_p^* \approx 0.3583 \pm 8.1\% \tag{28}$$

4.3 The Effect of Wedge Impact Velocity

In this section, in a constant wedge deadrise angle of 30 degrees, the effect of the wedge impact velocity for different velocities of 6.18, 9.79, 12.73, and 14.73 m/s is investigated. Figure 11 shows the dimensionless wedge

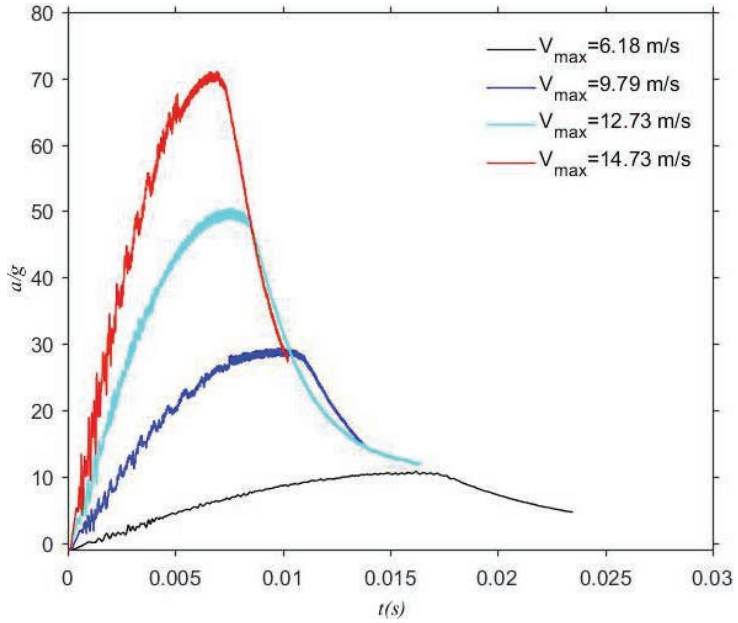

Figure 11 Dimensionless acceleration versus time for different impact velocities in the wedge deadrise angle of 30°.

acceleration versus time. Also, the free surface profile and the pressure contours are depicted in Appendix 1. According to Figure 11, increasing the wedge impact velocity increases the wedge acceleration while the time of reaching the maximum value decreases. Also, Figure 12 shows the slamming coefficient versus time and it is interesting to note that the maximum value of the slamming coefficient in all velocities is fairly the same, but in higher velocities, the maximum values occur sooner.

Using new Equations (18) and (23), Figure 11 can be re-sketched as in Figure 13 and it is depicted that all curves approximately coincide with each other and only the curve related to the impact velocity of 14.73 m/s has a little difference. Therefore, it can be assumed that the new dimensionless acceleration is independent of the impact velocity.

The maximum values of force, impact force coefficient, dimensionless acceleration, and related time of maximum force are tabulated in Table 3 and are used to derive the relations for calculating the peak values. According to Table 3, the maximum force exerted on the wedge increases and happens sooner when increasing the impact velocity. Similar to Table 2, some relations for the acceleration, impact force coefficient, and time of the peak load can be

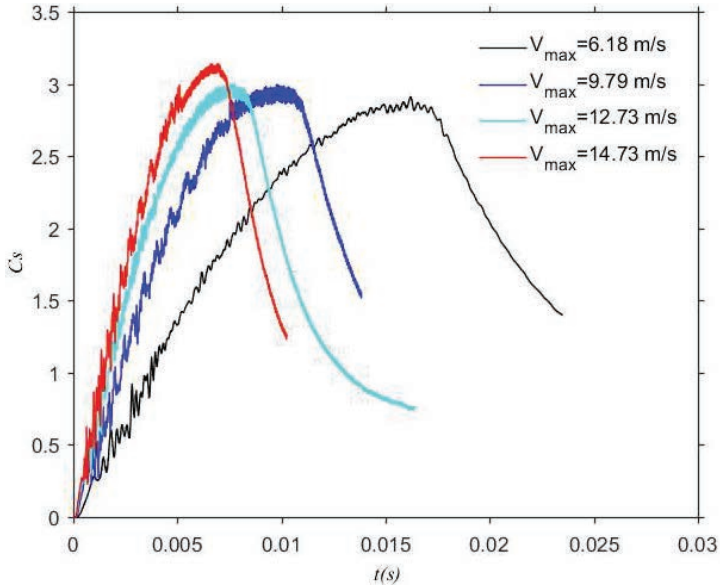

Figure 12 Slamming coefficient versus time for different impact velocities in the wedge deadrise angle of 30°.

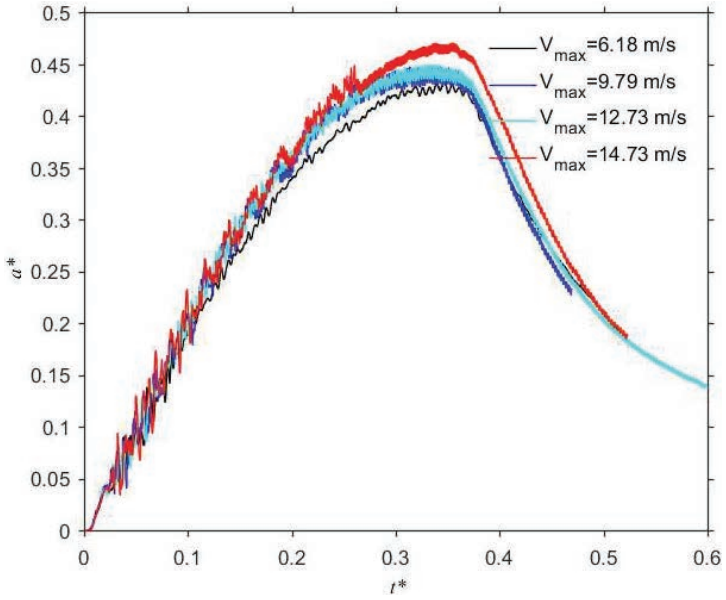

Figure 13 Dimensionless acceleration versus dimensionless time for different impact velocities in the wedge deadrise angle of 30°.

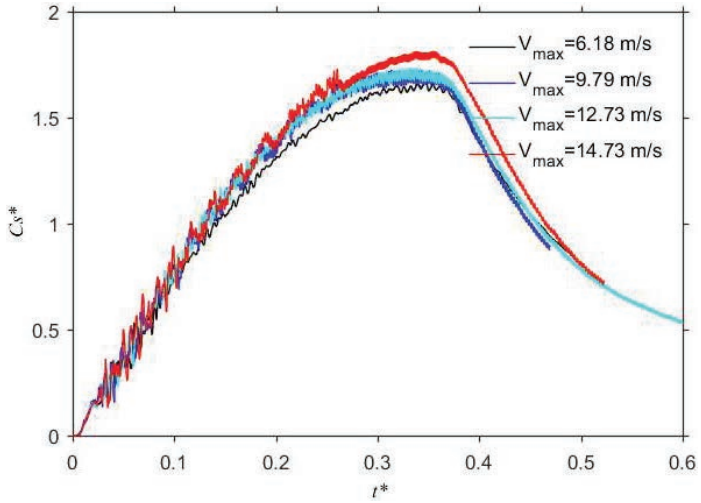

Figure 14 Impact force coefficient versus dimensionless time for different impact velocities in the wedge deadrise angle of 30°.

Table 3 Maximum force, impact force coefficient, and acceleration at the dimensionless time of the maximum force in the wedge angle of 30°

t_p^*	$F(KN)$	Cs_{max}^*	a_{max}^*	V_w (m/s)
0.346	5.56	1.68	0.436	6.18
0.331	14.356	1.73	0.448	9.79
0.339	24.32	1.735	0.449	12.73
0.355	34.11	1.815	0.470	14.73

derived from Table 3. Through averaging the values in Table 3, the following values are obtained with the maximum relative error of about 4 percent for the dimensionless acceleration, impact force coefficient, and the time of the maximum force respectively.

$$a_{max}^* \approx 0.451 \pm 4.25\% \tag{29}$$

$$Cs_{max}^* \approx 1.74 \pm 4.1\% \tag{30}$$

$$t_p^* \approx 0.3423 \pm 3.6\% \tag{31}$$

Table 4 Average values of impact force coefficient, dimensionless acceleration, and the dimensionless time of maximum impact force coefficient in different conditions

Conditions	t_p^*	Cs_{max}^*	a_{max}^*
Variable wedge angle	0.3583	1.7175	0.445
Variable velocity	0.3423	1.74	0.451
Average	0.350	1.729	0.448

4.4 The Unique Maximum Values

In this part, the results of Sections 4.2 and 4.3 are used to introduce average unique maximum values for three dimensionless parameters of a^*, Cs^*, and t^*. The first and second rows of Table 4 show the average values of these parameters in constant velocity with different wedge angles and constant deadrise wedge angle with different velocities, respectively. Also, the last row shows the average of these values from rows 1 and 2 as the final results.

Therefore, the final values of these parameters can be expressed as follows:

$$a_{max}^* \approx 0.448 \tag{32}$$

$$Cs_{max}^* \approx 1.729 \tag{33}$$

$$t_p^* \approx 0.350 \tag{34}$$

Now it is possible to obtain some equations for maximum acceleration and slamming coefficient by setting Equation (18) equal to $a_{max}^* \approx 0.448$ and Equation (19) equal to $Cs_{max}^* \approx 1.729$ respectively and it leads to Equations (35) and (36):

$$a_{max} = \frac{0.896V_w^2}{L_w tan(\theta)} - |g| \tag{35}$$

$$Cs_{max} = \frac{1.729}{tan(\theta)} \tag{36}$$

Equation (36) shows that the slamming coefficient is independent of the impact velocity.

Also by combining Equation (14) with Equation (36), the maximum force as in Equation (37) is obtained for the maximum force which is for a wedge with 1.0 m depth. Also one can obtain this equation by multiplying both sides of Equation (35) by the wedge mass.

$$F_{max} = 0.8645\frac{\rho_0 L_w V_w^2}{tan(\theta)} \tag{37}$$

Finally by setting Equation (23) equal to $t_p^* \approx 0.350$, Equation (38) can be obtained for the time of the peak load exerted on the wedge.

$$t_p = 0.35 \frac{L_w}{V_w} tan(\theta) \tag{38}$$

4.5 Introducing Unique Equations for the Dimensionless Parameters in a 2-D Wedge-Water Impact

Two parameters, the wedge deadrise angle θ, and the impact wedge velocity V_w are the premier parameters in investigating the wedge water entry problems. In this section general relations are proposed to calculate the most important parameters in the wedge water impact problems. In the previous sections, some relations and values are derived for acceleration, impact force coefficient, and the time when the peak load is exerted on the wedge. To derive these relations, at first, the wedge impact velocity is kept constant and the wedge angle is changed then the wedge angle is considered constant and the wedge impact velocity is varied. It is expected to have general relations for new dimensionless acceleration a^*, and dimensionless impact force Cs^* versus dimensionless time t^*. Therefore using curve-fitting techniques to all curves of constant velocities and constant wedge deadrise angles a unique and general relation for a^* and Cs^* versus t^* are presented in Equations (39) and (40):

$$a^* = \frac{-0.03449t^{*4} + 0.1139t^{*3} - 0.07211t^{*2} + 0.01365t^* - 0.00005024}{t^{*5} - 0.6189t^{*4} - 0.00984t^{*3} + 0.1145t^{*2} - 0.04703t^* + 0.007497} \tag{39}$$

$$Cs^* = \frac{-0.1031t^{*4} + 0.431t^{*3} - 0.2873t^{*2} + 0.05643t^* - 0.000197}{t^{*5} - 0.5116t^{*4} - 0.1081t^{*3} + 0.1474t^{*2} - 0.05248t^* + 0.008138} \tag{40}$$

Figures 15 and 16 show the comparison of the results of Equations (39) and (40) with experimental results of [35] which are non-dimensionalized using Equations (18), (19), and (23). They show good agreements between both curves until the maximum values, where they deviate from each other due to the three-dimensional effects.

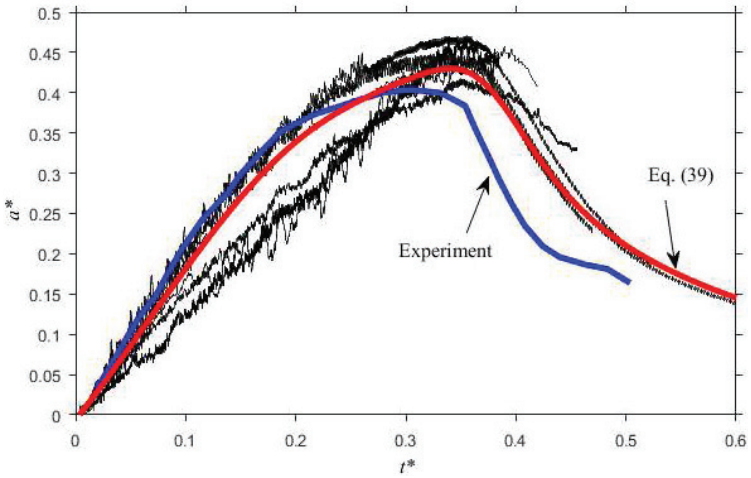

Figure 15 Comparison of the results of Equation (39) with the non-dimensionalized results of the present simulations and with the experiment [35].

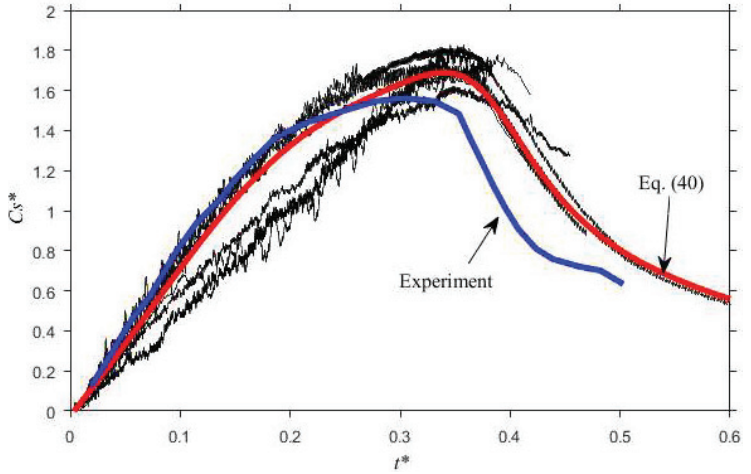

Figure 16 Comparison of the results of Equation (40) with the non-dimensionalized results of the present simulations and with the experiment [35].

5 Conclusion

At first, the present numerical method and the code are validated using the experimental and previous numerical results of two test cases of under-gate flow and wedge water entry problems. Then the effects of the wedge deadrise angle and the wedge impact velocity on the acceleration of the wedge and

the force which is exerted on the wedge are investigated. The results show that by reducing the wedge deadrise angle in a constant impact velocity the acceleration and the impact force increase. Also increasing the impact velocity in a constant wedge deadrise angle leads to an increase in the pressure, acceleration, and impact force. In the present study, some new dimensionless parameters are defined to find some general relations for expressing the dimensionless wedge impact force and dimensionless acceleration. These new parameters have been used in both cases of constant impact velocity with different wedge deadrise angles and constant wedge deadrise angles in different velocities for a 241 kg. There was a little difference between the coefficients due to round-off errors and curve fitting, therefore by combining these values using the averaging method, unique relations are achieved. Finally using all data, new and unique relations for the new dimensionless impact force and acceleration are presented and compared with experiments. It shows that these new relations can calculate the force and acceleration of a wedge water entry problem independent of wedge shape and velocity within the range of the conventional wedge shape, which is mostly used in marine architecture and for seaplanes. But in general, it is better not to use these relations at very high impact velocities, or deadrise angles close to zero or 90°. At these critical points, more research is needed to ensure the use of the proposed relations.

Appendix 1: Free surface deformation and the pressure distribution contours in the impact problem for different wedge deadrise angles and velocities.

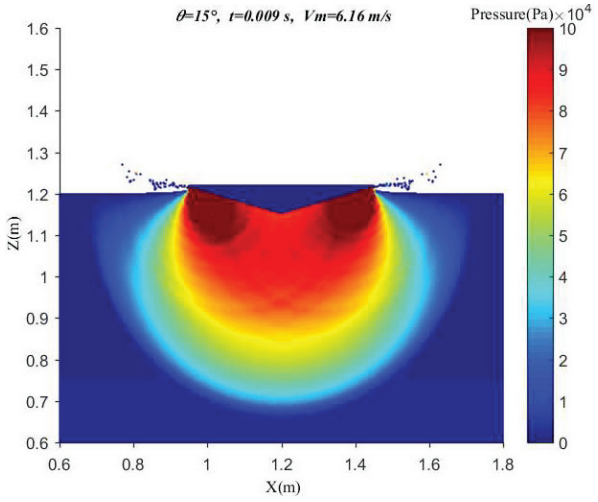

(a)

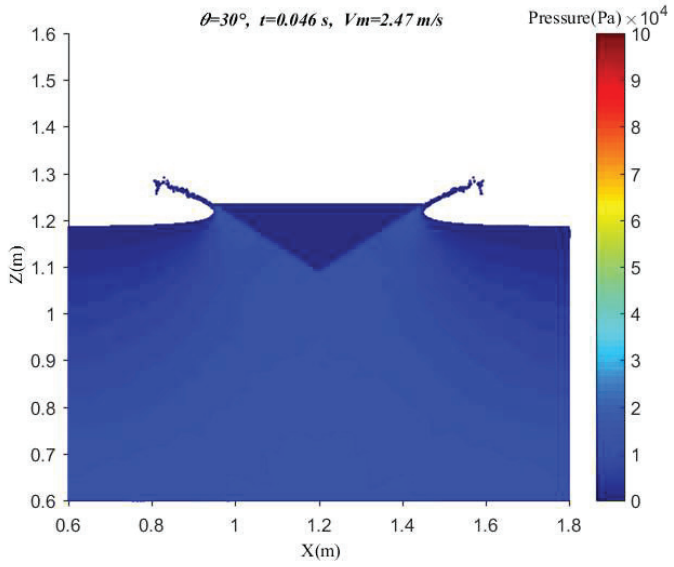
θ=30°, t=0.046 s, Vm=2.47 m/s
Pressure(Pa) × 10^4
Z(m)
X(m)

(b)

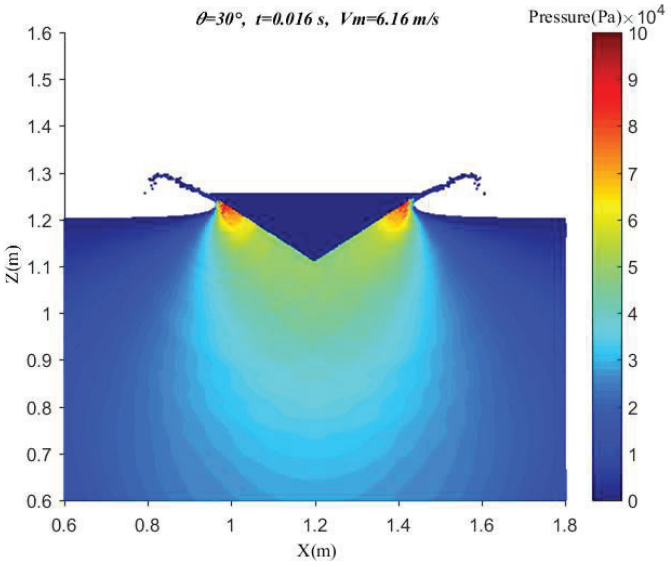
θ=30°, t=0.016 s, Vm=6.16 m/s
Pressure(Pa)× 10^4
Z(m)
X(m)

(c)

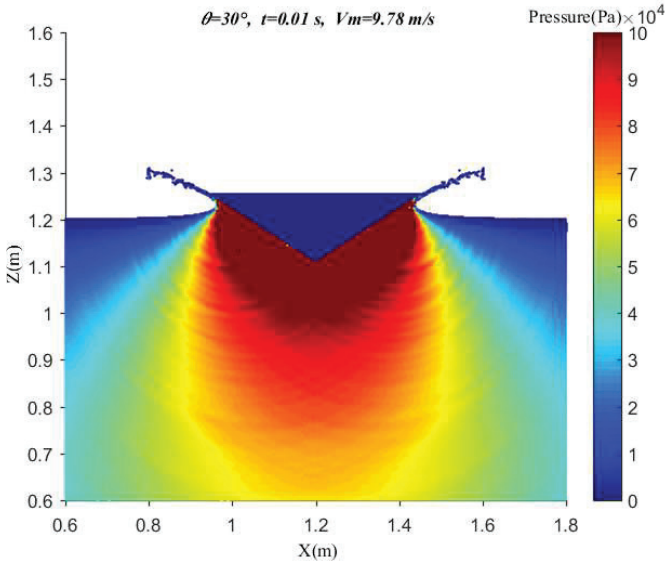
θ=30°, t=0.01 s, Vm=9.78 m/s
Pressure(Pa)×10^4
Z(m)
X(m)

(d)

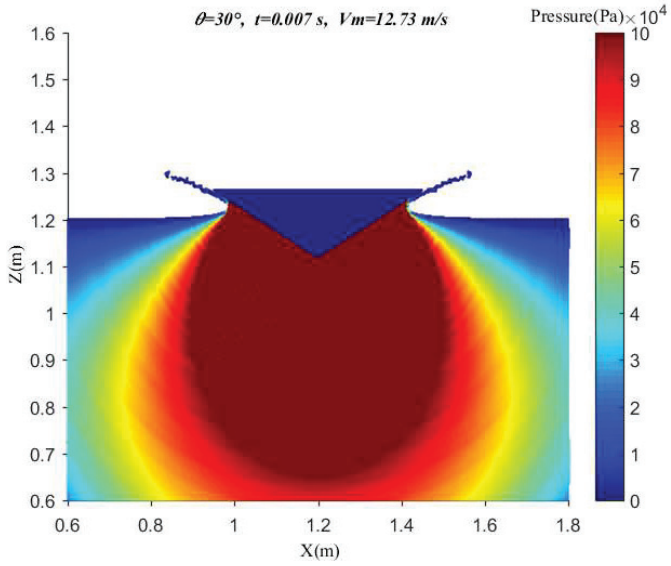
θ=30°, t=0.007 s, Vm=12.73 m/s
Pressure(Pa)×10^4
Z(m)
X(m)

(e)

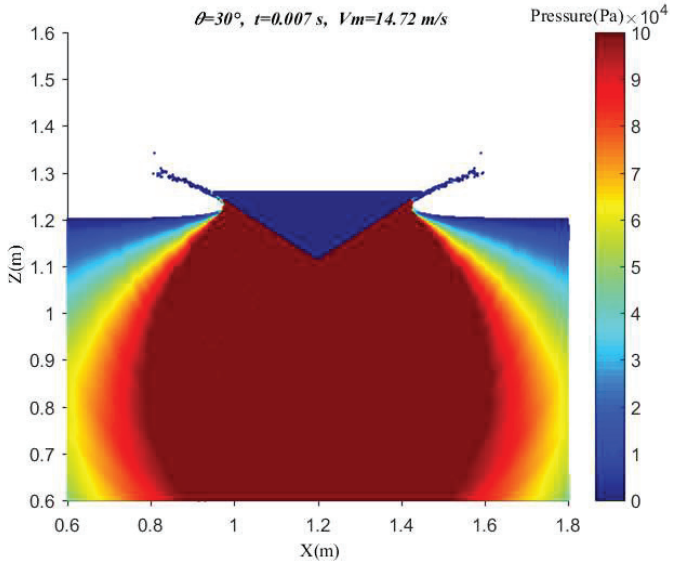
θ=30°, t=0.007 s, Vm=14.72 m/s
Pressure(Pa)×10^4
Z(m)
X(m)

(f)

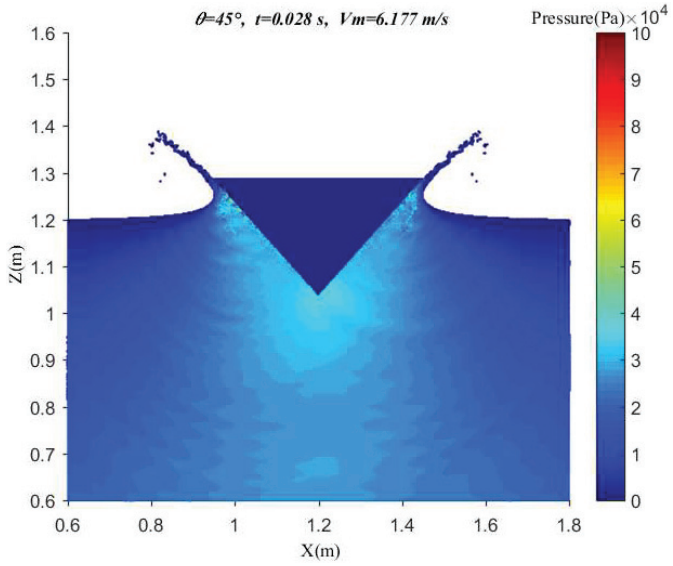
θ=45°, t=0.028 s, Vm=6.177 m/s
Pressure(Pa)×10^4
Z(m)
X(m)

(g)

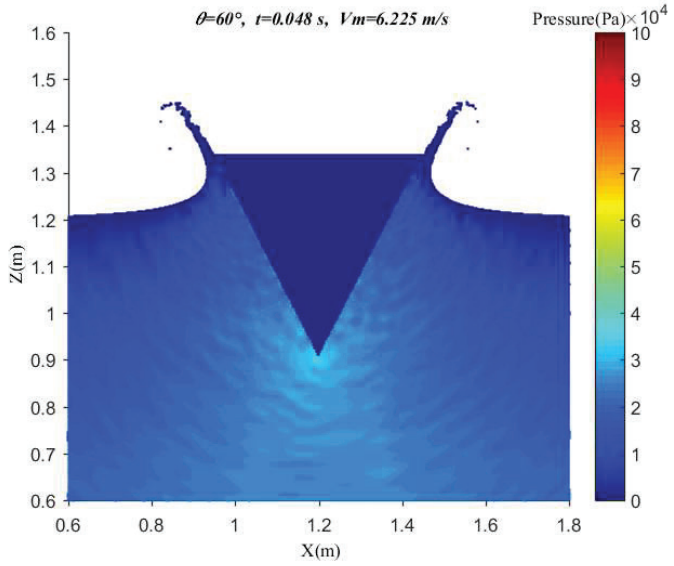

(h)

References

[1] H. Ghazizade-Ahsaee and A. Nikseresht, "Numerical solution of the asymmetric water impact of a wedge in three degrees of freedom," *China Ocean Engineering*, vol. 27, no. 3, pp. 313–322, 2013.

[2] T. Von Karman, "The impact on seaplane floats during landing," 1929.

[3] H. Wagner, "Über Stoß-und Gleitvorgänge an der Oberfläche von Flüssigkeiten," *ZAMM-Journal of Applied Mathematics and Mechanics/Zeitschrift für Angewandte Mathematik und Mechanik*, vol. 12, no. 4, pp. 193–215, 1932.

[4] Z. Dobrovol'Skaya, "On some problems of similarity flow of fluid with a free surface," *Journal of Fluid Mechanics*, vol. 36, no. 4, pp. 805–829, 1969.

[5] N. de Divitiis and L. M. de Socio, "Impact of floats on water," *Journal of Fluid Mechanics*, vol. 471, pp. 365–379, 2002.

[6] A. Korobkin, "Analytical models of water impact," *European Journal of Applied Mathematics*, vol. 15, no. 6, pp. 821–838, 2004.

[7] G. Logvinovich, "Hydrodynamics of flows with free boundaries," ed: Naukova Dumka, Kiev, 1969.

[8] L. B. Lucy, "A numerical approach to the testing of the fission hypothesis," *The astronomical journal*, vol. 82, pp. 1013–1024, 1977.

[9] R. A. Gingold and J. J. Monaghan, "Smoothed particle hydrodynamics: theory and application to non-spherical stars," *Monthly notices of the royal astronomical society*, vol. 181, no. 3, pp. 375–389, 1977.

[10] J. J. Monaghan, "Why particle methods work," *SIAM Journal on Scientific and Statistical Computing*, vol. 3, no. 4, pp. 422–433, 1982.

[11] J. Monaghan and R. Gingold, "Shock simulation by the particle method SPH," *Journal of computational physics*, vol. 52, no. 2, pp. 374–389, 1983.

[12] J. J. Monaghan and J. C. Lattanzio, "A refined particle method for astrophysical problems," *Astronomy and astrophysics*, vol. 149, pp. 135–143, 1985.

[13] J. Monaghan and H. Pongracic, "Artificial viscosity for particle methods," *Applied Numerical Mathematics*, vol. 1, no. 3, pp. 187–194, 1985.

[14] J. Lattanzio, J. Monaghan, H. Pongracic, and M. Schwarz, "Controlling penetration," *SIAM Journal on Scientific and Statistical Computing*, vol. 7, no. 2, pp. 591–598, 1986.

[15] J. Monaghan, "SPH meets the Shocks of Noh," *Monash University Paper*, 1987.

[16] J. J. Monaghan, "An introduction to SPH," *Computer physics communications*, vol. 48, no. 1, pp. 89–96, 1988.

[17] J. Monaghan, "On the problem of penetration in particle methods," *Journal of Computational physics*, vol. 82, no. 1, pp. 1–15, 1989.

[18] J. J. Monaghan, "Smoothed particle hydrodynamics," *Annual review of astronomy and astrophysics*, vol. 30, no. 1, pp. 543–574, 1992.

[19] J. J. Monaghan, "Simulating free surface flows with SPH," *Journal of computational physics*, vol. 110, no. 2, pp. 399–406, 1994.

[20] J. J. Monaghan, "SPH without a tensile instability," *Journal of Computational Physics*, vol. 159, no. 2, pp. 290–311, 2000.

[21] E.-M. Yettou, A. Desrochers, and Y. Champoux, "Experimental study on the water impact of a symmetrical wedge," *Fluid Dynamics Research*, vol. 38, no. 1, pp. 47–66, 2006.

[22] G. Oger, M. Doring, B. Alessandrini, and P. Ferrant, "Two-dimensional SPH simulations of wedge water entries," *Journal of computational physics*, vol. 213, no. 2, pp. 803–822, 2006.

[23] G. Kai, L. Hua, and B.-l. WANG, "Water entry of a wedge based on SPH model with an improved boundary treatment," *Journal of Hydrodynamics, Ser. B*, vol. 21, no. 6, pp. 750–757, 2009.
[24] K. Gong, B. Wang, and H. Liu, "Modelling water entry of a wedge by multiphase SPH method," *Coastal Engineering Proceedings*, vol. 1, no. 32, p. 10, 2011.
[25] P. K. Koukouvinis, J. S. Anagnostopoulos, and D. E. Papantonis, "Simulation of 2D wedge impacts on water using the SPH-ALE method," *Acta Mechanica*, vol. 224, no. 11, p. 2559, 2013.
[26] J. Vila, "On particle weighted methods and smooth particle hydrodynamics," *Mathematical models and methods in applied sciences*, vol. 9, no. 02, pp. 161–209, 1999.
[27] F. Sun, "Investigations of smoothed particle hydrodynamics method for fluid-rigid body interactions," University of Southampton, 2013.
[28] M. Farsi and P. Ghadimi, "Finding the best combination of numerical schemes for 2-D SPH simulation of wedge water entry for a wide range of deadrise angles," *International Journal of Naval Architecture and Ocean Engineering*, vol. 6, no. 3, pp. 638–651, 2014.
[29] A. Amicarelli, R. Albano, D. Mirauda, G. Agate, A. Sole, and R. Guandalini, "A Smoothed Particle Hydrodynamics model for 3D solid body transport in free surface flows," *Computers & fluids*, vol. 116, pp. 205–228, 2015.
[30] G. Chen and Y. Li, "Investigation of free surface flow in wedge water entry problem using Smoothed Particle Hydrodynamics method," in *OCEANS 2016-Shanghai*, 2016: IEEE, pp. 1–7.
[31] Y. Cheng, C. Ji, G. Zhai, and G. Oleg, "Numerical investigation of water entry of a wedge into waves with current effects using a fully nonlinear HOBEM," *Ocean Engineering*, vol. 153, pp. 33–52, 2018.
[32] Y. Chen, T. Khabakhpasheva, K. J. Maki, and A. Korobkin, "Wedge impact with the influence of ice," *Applied Ocean Research*, vol. 89, pp. 12–22, 2019.
[33] X. Wen, P. Liu, Q. Qu, and T. Hu, "Numerical and Theoretical Study on the Varying Speed Impact of Wedge Bodies on a Water Surface," *Journal of Fluids Engineering*, vol. 143, no. 1, 2021.
[34] X. Wen, P. Liu, Q. Qu, and T. Hu, "Impact of wedge bodies on wedge-shaped water surface with varying speed," *Journal of Fluids and Structures*, vol. 92, p. 102831, 2020.
[35] R. Zhao, O. Faltinsen, and J. Aarsnes, "Water entry of arbitrary two-dimensional sections with and without flow separation," in *Proceedings*

of the 21st symposium on naval hydrodynamics, 1996: Trondheim, Norway, National Academy Press, Washington, DC, USA, pp. 408–423.
[36] Z.-B. Wang, R. Chen, H. Wang, Q. Liao, X. Zhu, and S.-Z. Li, "An overview of smoothed particle hydrodynamics for simulating multiphase flow," *Applied Mathematical Modelling*, vol. 40, no. 23, pp. 9625–9655, 2016.
[37] A. Zhang, P. Sun, and F. Ming, "An SPH modeling of bubble rising and coalescing in three dimensions," *Computer Methods in Applied Mechanics and Engineering*, vol. 294, pp. 189–209, 2015.
[38] S. Farzin, Y. Hassanzadeh, M. T. Aalami, and R. Fatehi, "Development of Two Incompressible SPH methods to simulate sediment-laden free surface flows," *Modares Mechanical Engineering*, vol. 14, no. 12, 2015.
[39] J. P. Morris, P. J. Fox, and Y. Zhu, "Modeling low Reynolds number incompressible flows using SPH," *Journal of computational physics*, vol. 136, no. 1, pp. 214–226, 1997.
[40] M. Gesteira, B. Rogers, R. Dalrymple, A. Crespo, and M. Narayanaswamy, "User Guide for the SPHysics code," *University of Manchester, Manchester, UK*, 2010.
[41] H. Sabahi and A. Nikseresht, "Comparison of ISPH and WCSPH methods to solve fluid-structure interaction problems," *Scientia Iranica*, vol. 23, no. 6, pp. 2595–2605, 2016.
[42] A. H. Nikseresht and H. Ghazizade-Ahsaee, "Numerical simulation of three-dimensional dynamic motion of a standard NACA model in an impact problem," *International Journal of Engineering Systems Modelling and Simulation*, vol. 4, no. 4, pp. 190–194, 2012.

Biographies

Jafar Gerdabi received his B.Sc. and M.Sc. degrees from Birjand University and Shiraz University of Technology, Iran, in 2014 and 2017, respectively;

both in Mechanical Engineering. His research focuses on fluid-structure interaction problems, non-Newtonian fluids, and the smoothed particle hydrodynamics method. Analysis of numerical results in order to find out the general formulas with the help of dimensionless relations is one of his favourite activities in mathematics. He is also interested in computer programming.

Amir H. Nikseresht received his B.Sc., M.Sc., and Ph.D. from Shiraz University, Shiraz, Iran in 1995, 1997, and 2004, respectively, all in Mechanical Engineering. He is currently an Associate Professor of Mechanical Engineering at Shiraz University of Technology, Shiraz, Iran. His research interests include free surface flows, wave energy, CFD, hydrodynamics, and the smoothed particle hydrodynamics method.

Mohammad A. Esmaeili-Sikarudi received his Ph.D. in Mechanical Engineering from Shiraz University of Technology. His research interests involve two-phase modeling and the smoothed particle hydrodynamics method.